Correlation of Intraprostatic Tumor Extent with ^{68}Ga-PSMA Distribution in Patients with Prostate Cancer

Kambiz Rahbar[1], Matthias Weckesser[1], Sebastian Huss[2], Axel Semjonow[3], Hans-Jörg Breyholz[1], Andres J. Schrader[3], Michael Schäfers[1,4,5], and Martin Bögemann[3]

[1]Department of Nuclear Medicine, University Hospital Muenster, Muenster, Germany; [2]Gerhard Domagk Institute of Pathology, University Hospital Muenster, Muenster, Germany; [3]Prostate Center, Department for Urology, University Hospital Muenster, Muenster, Germany; [4]European Institute for Molecular Imaging, University of Muenster, Muenster, Germany; and [5]Cells-in-Motion Cluster of Excellence, University of Muenster, Muenster, Germany

We evaluated the diagnostic value and accuracy of prostate-specific membrane antigen (PSMA) PET for the intraprostatic delineation of prostate cancer before prostatectomy. **Methods:** We identified 6 patients with biopsy-proven high-risk prostate cancer who were referred for ^{68}Ga-PSMA PET/CT before radical prostatectomy to rule out metastasis. After prostatectomy, a histologic map of the prostate was reconstructed. The histologic extent and Gleason score of each segment of the prostate were compared with ^{68}Ga-PSMA PET images resliced to the histologic axis. Sensitivity, specificity, positive and negative predictive value, and positive and negative likelihood ratios were calculated. The SUV of each segment was measured, and median values were compared. **Results:** Of the 132 segments, 112 were eligible for analysis. The correlation of histologic results with ^{68}Ga-PSMA PET images showed a specificity and sensitivity of 92%. The positive and negative likelihood ratio and the positive and negative predictive value for detection of prostate cancer on ^{68}Ga-PSMA PET were 11.5, 0.09, 96%, and 85%, respectively. The median SUV_{max} of true-positive prostate segments was significantly higher than that of true-negative segments (11.0 ± 7.8 vs. 2.7 ± 0.9, $P < 0.001$), and a cutoff of 4 revealed a sensitivity and specificity of 86.5% and an accuracy of 87.5%. **Conclusion:** These preliminary results show that the intraprostatic localization and extent of prostate cancer may be estimated by ^{68}Ga-PSMA PET. This imaging method may be helpful for identifying target lesions before prostate biopsy and may support decision making before focal or radical therapy.

Key Words: PSMA PET/CT; prostate cancer; pilot study; prostatectomy

J Nucl Med 2016; 57:563–567
DOI: 10.2967/jnumed.115.169243

Prostate cancer is the most common cancer in men. Within the United States, an estimated 26% of cancer cases in 2015 were expected to be prostate cancer (*1*). Prostate-specific antigen–based screening leads to a significant proportion of overdiagnosis (*2*) and, consequently, overtreatment (*3*). Overtreatment is partly caused by an unknown true tumor extent before prostate biopsy and by the planning of a definitive therapy.

Prostate-specific membrane antigen (PSMA) is a transmembrane protein (*4*) expressed in prostate epithelial cells. Its expression is increased in prostate cancer cells and becomes higher as the cancer progresses (*5,6*). PSMA is also expressed in some normal tissues (e.g., small intestine, renal tubules, and salivary glands) (*7*), but in prostate cancer the expression levels are 100- to 1,000-fold higher (*8*). Some recently developed ^{68}Ga-labeled PSMA ligands have been shown to have high specificity and sensitivity for the detection of recurrent prostate cancer and metastatic disease (*9*).

PSMA-based imaging may have the potential to exactly characterize the extent of intraprostatic disease and may therefore be a useful tool to identify and define malignant lesions before prostate biopsy and, finally, to help tailor an optimal, definitive therapy for each patient. Therefore, the aim of this proof-of-concept study was to analyze the performance of ^{68}Ga-labeled ^{68}Ga-PSMA PET/CT for prediction of the true extent of cancer within the prostate and seminal vesicles.

MATERIALS AND METHODS

Patient Population

Between May 2014 and August 2015, we identified 6 patients (mean age ± SD, 65 ± 8.2 y; range, 56–73 y) with biopsy-proven prostate cancer who had undergone ^{68}Ga-PSMA PET/CT 3–32 d before radical prostatectomy (RPE) because of a high risk of extraprostatic manifestation of prostate cancer. Transrectal ultrasound–guided prostate biopsy with 6–14 cores had been performed for all patients. Local and external reference pathology institutions performed histologic analysis and Gleason scoring. ^{68}Ga-PSMA PET/CT was performed to rule out metastasis. The indication for ^{68}Ga-PSMA imaging was appointed by an interdisciplinary tumor board. All patients signed an informed consent form before undergoing PET/CT.

In 2 patients, metastasis was found (a single bone metastasis in one patient and nodal involvement in the other patient). There is increasing evidence that even in patients with lymph node involvement or a few bone lesions, RPE may delay progression, delay castration-resistant cancer, and even prolong survival (*10,11*). These available data were thoroughly clarified for the 2 patients with metastasis, and they were then offered the possibility of RPE. Both patients consented to it. The institutional review board approved this retrospective study, and the requirement to obtain informed consent was waived.

Patient Preparation and ^{68}Ga-PSMA PET/CT

Whole-body PET/CT was performed 65.1 ± 7.0 min after injection of 161 ± 19.8 MBq (range, 131–193 MBq) of ^{68}Ga-PSMA-HBED-CC

Received Nov. 4, 2015; revision accepted Dec. 4, 2015.
For correspondence or reprints contact: Kambiz Rahbar, Department of Nuclear Medicine, University Hospital Muenster, Albert-Schweitzer-Campus 1, 48149 Muenster, Germany.
E-mail: rahbar@uni-muenster.de
Published online Jan. 14, 2016.

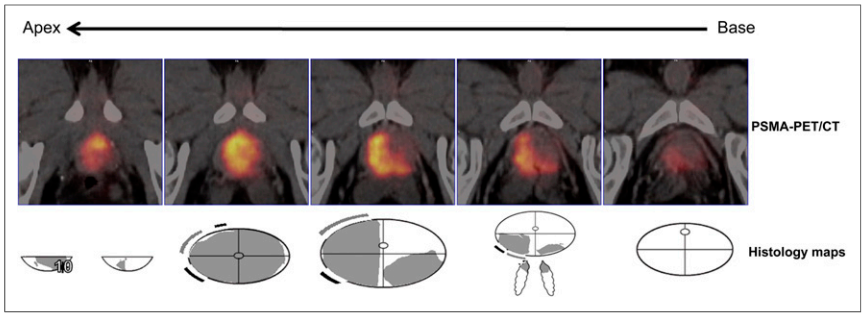

FIGURE 1. Reangulated slices from patient 1 show concordance between ^{68}Ga-PSMA distribution and histologic maps. "10" represents 10-mm positive surgical margin.

(HBED-CC is *N,N′*-bis[2-hydroxy-5(carboxyethyl)benzyl]ethylenediamine-*N,N′*-diacetic acid) (*12*). The patients were asked to void immediately before undergoing scanning. The scans were obtained using a high-resolution hybrid PET/CT system (Biograph mCT, with a 128-slice CT component; Siemens Medical Solutions). Low-dose CT of the entire area covered by PET (from skull to mid-thigh) was performed for attenuation correction. After completion of the CT scan, PET data were acquired for 3 min per bed position. PET images were reconstructed using the standard manufacturer-supplied software (PET resolution of 3 mm).

Image Analysis

Two board-certified radiologists and nuclear medicine physicians clinically analyzed the images before RPE. SUV_{max} was measured within each prostate segment after reangulation of the images to match the histologic slices of the prostate, which were from base to apex and axial to the course of the urethra. A board-certified urologist, nuclear medicine physician, and pathologist compared the ^{68}Ga-PSMA images with the postoperative histologic maps to determine whether the imaging findings for each prostate segment were true-positive, true-negative, false-positive, or false-negative.

Pathologic Evaluation

RPE was performed on all 6 patients. The prostate specimens were processed and evaluated according to the local standard operating procedures of the Institute of Pathology (*13*). After macroscopic examination, the prostate and seminal vesicles were fixed in 10% neutral buffered 4% formalin solution (~4% formaldehyde). The gland was prepared for histology by a modified version of the technique introduced by the Association of Clinical Pathologists (*14*). After removal of the apex and base of the prostate, the gland was cut transversally into 5-mm-thick slices. Finally, the slices were separated into right and left halves and front and back sections. The complete slices of the specimen were embedded in paraffin blocks, which were then cut into 4-μm slices, stained with hematoxylin and eosin, and microscopically examined. The Gleason score (*15*) and the stage were determined according to the Union International Contre le Cancer and TNM systems (*16*).

Topographic Analysis

The extent of cancer within the specimen was mapped according to the method Bettendorf et al. (*13*) and Eminaga et al. (*17*). The map consists of 22 segments, including 2 segments for the seminal vesicles. The digitized data were the basis for calculation of percentage tumor volume. The Gleason score of each segment was individually documented. An example map is shown in Figure 1.

Statistical Analysis

SPSS Statistics, version 23 (IBM), was used for analysis. Sensitivity, specificity, positive and negative predictive value, and positive and negative likelihood ratios were calculated for all available segments. A Kruskal–Wallis test was performed to compare the median SUV_{max} of true-positive and true-negative segments. We estimated the diagnostic performance of ^{68}Ga-PSMA PET by calculating the area under the receiver-operating-characteristic curve. Two-sided P values of less than 0.05 were considered statistically significant.

RESULTS

Histologic results were available for 132 segments from 6 patients. For each patient, the analysis excluded 2 segments that could not be identified on PET/CT compared with the anatomy of the prostate. In 2 patients (patients 2 and 5), 4 segments adjacent to the bladder were excluded because of spillover of urine activity. Thus, a total of 112 segments were included in the statistical analysis.

Detailed clinical data and histopathologic results for the patients are summarized in Table 1.

Comparison of Cancer Maps, Gleason Scores, and ^{68}Ga-PSMA PET Results

Only 3 of 37 segments without histologic cancer on the maps were considered positive on the corresponding slices from ^{68}Ga-PSMA PET, resulting in a specificity of 92% (Table 2). With the maps being defined as the gold standard, the sensitivity of ^{68}Ga-PSMA PET for identifying areas with cancer was 92%. Of the 3 false-positive segments, one showed active prostatitis, one chronic prostatitis, and one high-grade prostatic intraepithelial neoplasia.

The positive and negative likelihood ratios for ^{68}Ga-PSMA PET in detecting prostate cancer were 11.5 and 0.09, respectively. The positive and negative predictive values were 96% and 85%, respectively, indicating a strong and exact correlation between ^{68}Ga-PSMA positivity and the actual histologic presence of cancer. SUV_{max} was significantly higher for true-positive segments than for true-negative segments (median, 11.0 ± 7.8 vs. 2.7 ± 0.9; $P <$ 0.001; Kruskal–Wallis test).

An analysis of the area under the receiver-operating-characteristic curve for SUV_{max} (Fig. 2) in correlation with the histologic results revealed an area under the curve of 0.93 (95% confidence interval, 0.89–0.99; $P < 0.001$). Using an SUV_{max} cutoff of 4.0, a sensitivity and specificity of 88% and 86.5% and an accuracy of 87.5% were achieved.

Comparison of Gleason scores and ^{68}Ga-PSMA PET results (Fig. 3) showed a high detection rate for true-positive segments (80%), even in lower Gleason scores of 3 + 3 = 6.

The box plot of SUV_{max} against Gleason score showed a tendency of SUV_{max} to increase, but because of the small number of patients no statistical analysis was performed (Fig. 3).

DISCUSSION

Preoperative information on the localization and extent of cancer within the prostate is limited, still lacks accuracy, and may result in inappropriate treatment (*18*). Multiparametric MRI is being increasingly used to display the local tumor burden within the prostate. However, despite its ability to detect lesions with a Gleason score of 7 or higher, especially in larger tumor foci, it has clinically significant limitations in smaller lesions and lesions with a Gleason score of less than 7. In a study in which multiparametric

TABLE 1
Pre- and Postoperative Patient Characteristics

Characteristic	Patient 1	Patient 2	Patient 3	Patient 4	Patient 5	Patient 6
Age (y)	59	57	73	72	73	56
Initial PSA level (ng/mL)	111.1	5.7	27.0	30.6	9.6	76.3
Prostate biopsy						
Gleason score	4 + 3 = 7b	3 + 4 = 7a	3 + 4 = 7a	4 + 3 = 7b	3 + 4 = 7a	8
Cancer location	R < L	R > L	R = L	L only	R > L	R = L
Number of positive cores	6/10	5/8	5/6	3/12	7/10	11/11
Clinical stage	cT2c (L lobe)	cT2a (R base)	cT1	cT1	cT2c (bilateral)	cT2c (both lobes)
TRUS suggestive of cancer	L lobe	R base	Normal	Normal	R base	Both lobes
TRUS prostate volume (cm^3)	36	40	36	39	17	49
Staging						
Bone scan indication	Not done (PSMA PET)	Routine scan	PSA elevation	Not done (PSMA PET)	Routine scan	Not done (PSMA PET)
Bone scan result		L os ilium lesion	Exclusion of mets		L3 lesion	
^{68}Ga-PSMA PET indication	Exclusion of mets	Suggestive bone scan	Exclusion of mets	Exclusion of mets	Exclusion of mets	Exclusion of mets
^{68}Ga-PSMA PET result	Parailiac LN mets	Equivocal*	No lesions	No lesions	No lesions	LN mets†
RPE						
Prostate volume (cm^3)	48	34	40	52	30	51
Cancer volume (cm^3)	20.9	2.6	5.7	14.5	7.8	30.2
Cancer involvement	43.5%	7.8%	14.6%	27.9%	26.5%	59.2%
Gleason score	4 + 3 = 7b	3 + 4 = 7a	4 + 3 = 7b	4 + 3 = 7b	4 + 5 = 9a	4 + 5 = 9a
Positive surgical margin	L apex	No	R anterior	L seminal vesicle	No	L posterior
Seminal vesicle invasion	Both	L	No	L	Both	Both
Pathologic stage	pT3b pN1	pT3b pN0	pT3a pN0	pT3b pN1	pT3b pN0	pT3b N1

*Possible bony lesion.
†Iliac, aortal, and pararectal.
PSA = prostate-specific antigen; TRUS = transrectal ultrasound; mets = metastasis; LN = lymph node.

MRI was performed before RPE and correlated with the true tumor extent, Le et al. found that 80% of tumors were detected. However, tumors with a diameter smaller than 1 cm were missed by multiparametric MRI in most cases, even in some cases of high-grade lesions. Lesions with a Gleason score of 6 were missed in 80% of cases regardless of the diameter of the lesions (*19*).

In contrast, the specificity and sensitivity of ^{68}Ga-PSMA PET in prostate cancer is reliable even when the Gleason score is 6 or less (*9*). The present preliminary analysis compared preoperative ^{68}Ga-PSMA PET/CT imaging with postoperative cancer maps of the prostate. The results indicated high accuracy in predicting the pattern of cancer growth in the prostate by regional ^{68}Ga-PSMA uptake.

To our knowledge, there have been only 2 publications reporting PSMA uptake in the prostate before RPE (*20,21*). Budäus et al. reported only about the use of ^{68}Ga-PSMA to visualize cancer in the prostate gland (*20*). Using a 12-segment model, Rowe et al. showed a poor sensitivity of 10% and accuracy of 56% for detection of malignant prostate lesions in a stringent analysis of an ^{18}F-labeled PSMA tracer (^{18}F-DCFBC, or *N*-[*N*-[(*S*)-1,3-dicarboxypropyl]carbamoyl]-4-^{18}F-fluorobenzyl-L-cysteine) that has a lower tumor-to-background contrast than ^{68}Ga-PSMA-HBED-CC and seems to have a lower capability (*21*). In the same patient cohort and using the same stringent analysis, multiparametric MRI had a sensitivity of 35% and accuracy of 62%. In contrast, in applying ^{68}Ga-PSMA PET imaging, we found a high sensitivity of 92% and accuracy of 92% in detecting malignant lesions using a 22-segment model. This discrepancy between our results and those of Rowe et al. might be explained not only by the superior tumor-to-background contrast of

TABLE 2
^{68}Ga-PSMA vs. Histology Results for Segments Verified Histopathologically After RPE

^{68}Ga-PSMA result	Histology result	
	Positive (n = 75)	Negative (n = 37)
Positive (n = 72)	69	3
Negative (n = 40)	6	34

Sensitivity, 92% (95% confidence interval, 0.83–0.97); specificity, 92% (95% confidence interval, 0.77–0.98); accuracy, 92%; positive predictive value, 96%; negative predictive value, 85%.

^{68}Ga-PSMA-HBED-CC but by the fact that reangulation of our images matched the histologic workup, in which the prostate was sliced axially to the urethra. A curved reangulation might match the histologic slices even better and should be evaluated in further studies.

Furthermore, in line with the results of Rowe et al. (*21*), our results indicated a significantly higher uptake in malignant lesions than in cancer-free segments (median SUV_{max}, 11.0 ± 7.8 vs. 2.7 ± 0.9; $P < 0.001$). However, their study found a lower SUV_{max} using an ^{18}F-labeled PSMA tracer (median SUV_{max}, 3.5 vs. 2.2; $P = 0.004$).

In the present study, we thoroughly correlated histopathologic findings with ^{68}Ga-PSMA PET findings and were able to confirm the results of a recent study by Afshar-Oromieh et al., who found that ^{68}Ga-PSMA-HBED-CC is also reliable in the detection of prostate cancer that has a low Gleason score (≤7) (*9*).

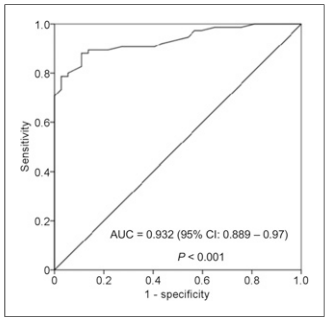

FIGURE 2. Area under receiver-operating-characteristic curve (AUC) for SUV_{max} according to histologic results. CI = confidence interval.

Recent publications have demonstrated the increasing importance of using ^{68}Ga-PSMA imaging to determine local recurrence or metastasis of prostate cancer (*9,12,21*). However, the decision to use ^{68}Ga-PSMA imaging to rule out metastatic disease before prostatectomy must be made with caution and with an awareness of the patient's disease history and of the potential for false-positive findings. For example, recent studies and case reports have shown high ^{68}Ga-PSMA uptake in such conditions as schwannomas, celiac ganglia, and even differentiated thyroid cancer (*22–24*).

Our study was limited by deficiencies inherent in the retrospective approach and the small number of patients. In addition, to avoid spillover from urine activity, an indwelling catheter to empty the bladder before imaging could have been used. Despite these limitations, the present findings are a strong indication that the information provided by cross-sectional ^{68}Ga-PSMA PET imaging may help clarify the localization and extent of cancer within the prostate both before biopsy and before definitive therapy. In particular, this novel technique has the potential to significantly improve decision making on the optimal, definitive therapy for individual patients. If our results are confirmed in larger collectives, ^{68}Ga-PSMA PET imaging may help in decisions on whether to use focal treatment or radical treatment and—for RPE—on whether to use a nerve-sparing approach or a wide excision.

The data presented here are currently being validated. Optimization of the imaging protocols, such as through dynamic acquisition and dual-time-point imaging, seems to improve sensitivity further by further increasing the contrast of ^{68}Ga-PSMA activity.

CONCLUSION

This preliminary proof-of-concept study showed that the localization and extent of cancer within the prostate can be estimated with high accuracy by ^{68}Ga-PSMA PET technology. Therefore, this imaging method may be helpful for identifying target lesions before prostate biopsy and may support decision making on focal versus radical therapy. Larger studies with dedicated imaging protocols are needed to further evaluate the significance of these data, especially with use of hybrid imaging systems such as PET/MRI.

DISCLOSURE

The costs of publication of this article were defrayed in part by the payment of page charges. Therefore, and solely to indicate this fact, this article is hereby marked "advertisement" in accordance with 18 USC section 1734. No potential conflict of interest relevant to this article was reported.

ACKNOWLEDGMENT

We thank the PET radiochemistry group at the Department of Nuclear Medicine for highly reliable production of ^{68}Ga-PSMA, as well as the PET/CT radiographers for excellent technical assistance.

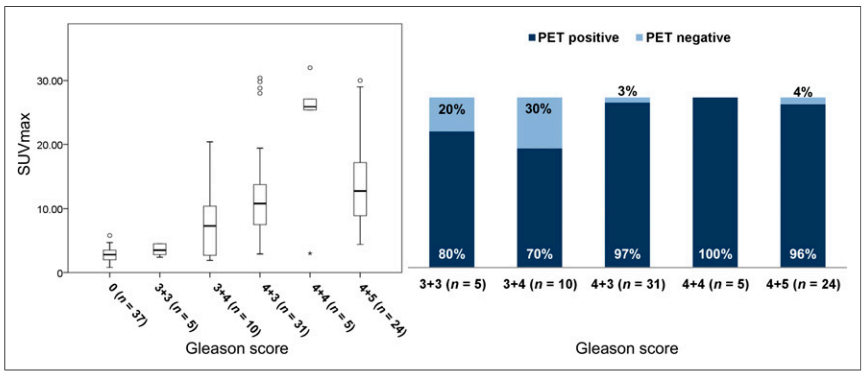

FIGURE 3. Graph on left plots SUV_{max} according to different locoregional Gleason scores. Graph on right depicts detection rates for segments true-positive on ^{68}Ga-PSMA PET.

REFERENCES

1. Siegel RL, Miller KD, Jemal A. Cancer statistics, 2015. *CA Cancer J Clin.* 2015;65:5–29.
2. Etzioni R, Gulati R, Mallinger L, Mandelblatt J. Influence of study features and methods on overdiagnosis estimates in breast and prostate cancer screening. *Ann Intern Med.* 2013;158:831–838.
3. Wilt TJ, Brawer MK, Barry MJ, et al. The Prostate Cancer Intervention Versus Observation Trial: VA/NCI/AHRQ Cooperative Studies Program #407 (PIVOT): design and baseline results of a randomized controlled trial comparing radical prostatectomy to watchful waiting for men with clinically localized prostate cancer. *Contemp Clin Trials.* 2009;30:81–87.

4. Davis MI, Bennett MJ, Thomas LM, Bjorkman PJ. Crystal structure of prostate-specific membrane antigen, a tumor marker and peptidase. *Proc Natl Acad Sci USA.* 2005;102:5981–5986.
5. Wright GL Jr, Grob BM, Haley C, et al. Upregulation of prostate-specific membrane antigen after androgen-deprivation therapy. *Urology.* 1996;48:326–334.
6. Ross JS, Sheehan CE, Fisher HA, et al. Correlation of primary tumor prostate-specific membrane antigen expression with disease recurrence in prostate cancer. *Clin Cancer Res.* 2003;9:6357–6362.
7. Troyer JK, Beckett ML, Wright GL Jr. Detection and characterization of the prostate-specific membrane antigen (PSMA) in tissue extracts and body fluids. *Int J Cancer.* 1995;62:552–558.
8. Sokoloff RL, Norton KC, Gasior CL, Marker KM, Grauer LS. A dual-monoclonal sandwich assay for prostate-specific membrane antigen: levels in tissues, seminal fluid and urine. *Prostate.* 2000;43:150–157.
9. Afshar-Oromieh A, Avtzi E, Giesel FL, et al. The diagnostic value of PET/CT imaging with the ^{68}Ga-labelled PSMA ligand HBED-CC in the diagnosis of recurrent prostate cancer. *Eur J Nucl Med Mol Imaging.* 2015;42:197–209.
10. Heidenreich A, Pfister D, Porres D. Cytoreductive radical prostatectomy in patients with prostate cancer and low volume skeletal metastases: results of a feasibility and case-control study. *J Urol.* 2015;193:832–838.
11. Neugut AI, Gelmann EP. Treatment of the prostate in the presence of metastases: lessons from other solid tumors. *Eur Urol.* June 19, 2015 [Epub ahead of print].
12. Afshar-Oromieh A, Haberkorn U, Eder M, Eisenhut M, Zechmann CM. [^{68}Ga] gallium-labelled PSMA ligand as superior PET tracer for the diagnosis of prostate cancer: comparison with ^{18}F-FECH. *Eur J Nucl Med Mol Imaging.* 2012;39:1085–1086.
13. Bettendorf O, Oberpenning F, Kopke T, et al. Implementation of a map in radical prostatectomy specimen allows visual estimation of tumor volume. *Eur J Surg Oncol.* 2007;33:352–357.
14. Association of Clinical Pathologists. Guidelines for the macroscopic processing of radical prostatectomy and pelvic lymphadenectomy specimens. *J Clin Pathol.* 2008;61:713–721.
15. Epstein JI, Allsbrook WC Jr, Amin MB, Egevad LL. Update on the Gleason grading system for prostate cancer: results of an international consensus conference of urologic pathologists. *Adv Anat Pathol.* 2006;13:57–59.
16. Sobin LH, Gospodarowicz MK, Wittekind C, eds. *TNM Classification of Malignant Tumours.* 7th ed. Hoboken, NJ: Wiley-Blackwell; 2010.
17. Eminaga O, Hinkelammert R, Semjonow A, et al. Clinical map document based on XML (cMDX): document architecture with mapping feature for reporting and analysing prostate cancer in radical prostatectomy specimens. *BMC Med Inform Decis Mak.* 2010;10:71.
18. Busch J, Magheli A, Leva N, et al. Higher rates of upgrading and upstaging in older patients undergoing radical prostatectomy and qualifying for active surveillance. *BJU Int.* 2014;114:517–521.
19. Le JD, Tan N, Shkolyar E, et al. Multifocality and prostate cancer detection by multiparametric magnetic resonance imaging: correlation with whole-mount histopathology. *Eur Urol.* 2015;67:569–576.
20. Budäus L, Leyh-Bannurah SR, Salomon G, et al. Initial experience of Ga-PSMA PET/CT imaging in high-risk prostate cancer patients prior to radical prostatectomy. *Eur Urol.* June 24, 2015 [Epub ahead of print].
21. Rowe SP, Gage KL, Faraj SF, et al. ^{18}F-DCFBC PET/CT for PSMA-based detection and characterization of primary prostate cancer. *J Nucl Med.* 2015; 56:1003–1010.
22. Ripschler C, Maurer T, Schwaiger M, Eiber M. Intense PSMA-expression using ^{68}Ga-PSMA PET/CT in a paravertebral schwannoma mimicking prostate cancer metastasis. *Eur J Nucl Med Mol Imaging.* 2016;43:193–194.
23. Krohn T, Verburg FA, Pufe T, et al. ^{68}Ga-PSMA-HBED uptake mimicking lymph node metastasis in coeliac ganglia: an important pitfall in clinical practice. *Eur J Nucl Med Mol Imaging.* 2015;42:210–214.
24. Verburg FA, Krohn T, Heinzel A, Mottaghy FM, Behrendt FF. First evidence of PSMA expression in differentiated thyroid cancer using ^{68}Ga-PSMA-HBED-CC PET/CT. *Eur J Nucl Med Imaging.* 2015;42:1622–1623.